

Serveur Académique Lausannois SERVAL serval.unil.ch

Author Manuscript

Faculty of Biology and Medicine Publication

This paper has been peer-reviewed but does not include the final publisher proof-corrections or journal pagination.

Published in final edited form as:

Title: OATPB1/B3 and MRP3 expression in hepatocellular adenoma predicts Gd-EOB-DTPA uptake and correlates with risk of malignancy.

Authors: Sciarra A, Schmidt S, Pellegrinelli A, Maggioni M, Dondossola D, Pasquier J, Cigala C, Tosi D, Halkic N, Bulfamante G, Viale G, Bosari S, Balabaud C, Bioulac-Sage P, Sempoux C

Journal: Liver international : official journal of the International Association for the Study of the Liver

Year: 2019 Jan

Issue: 39

Volume: 1

Pages: 158-167

DOI: [10.1111/liv.13964](https://doi.org/10.1111/liv.13964)

In the absence of a copyright statement, users should assume that standard copyright protection applies, unless the article contains an explicit statement to the contrary. In case of doubt, contact the journal publisher to verify the copyright status of an article.

DR. AMEDEO SCIARRA (Orcid ID : 0000-0002-7550-0312)

PROF. CHARLES BALABAUD (Orcid ID : 0000-0003-0081-8112)

Article type : Original Articles

Editor: Francesco Negro

OATPB1/B3 and MRP3 expression in hepatocellular adenoma predicts Gd-EOB-DTPA uptake and correlates with risk of malignancy

Amedeo Sciarra^{1,2}; Sabine Schmidt³; Alessandro Pellegrinelli⁴; **Marco Maggioni**²;
Daniele Dondossola⁵; Jerome Pasquier⁶; Claudia Cigala⁷; Delfina Tosi⁷; Nermin Halkic⁸ Gaetano Bulfamante⁷; Giuseppe Viale⁹; Silvano Bosari²; Charles Balabaud¹⁰;
Paulette Bioulac-Sage¹⁰; Christine Sempoux¹

1. Service of Clinical Pathology, Lausanne University Hospital, Institute of Pathology, Lausanne, Switzerland
2. Pathology, Fondazione IRCCS Ca' Granda-Ospedale Maggiore Policlinico, University of Milan, Milan, Italy
3. Department of Diagnostic and Interventional Radiology, Lausanne University Hospital, Lausanne, Switzerland
4. Pathology Department, Fondazione IRCCS Istituto Nazionale Tumori, Milan, Italy.
5. Liver Transplant and General Surgery Unit, Fondazione IRCCS Ca' Granda-Ospedale Maggiore Policlinico, Milan, Italy
6. Institute for Social and Preventive Medicine, Lausanne University Hospital, Lausanne, Switzerland

This article has been accepted for publication and undergone full peer review but has not been through the copyediting, typesetting, pagination and proofreading process, which may lead to differences between this version and the Version of Record. Please cite this article as doi: 10.1111/liv.13964

This article is protected by copyright. All rights reserved.

7. Unit of Pathology, San Paolo Hospital Medical School, Department of Health Sciences, University of Milan, Milan, Italy
8. Department of Visceral Surgery, Lausanne University Hospital, Lausanne, Switzerland.
9. European Institute of Oncology, University of Milan, Milan, Italy
10. Pathology Department, CHU de Bordeaux, Pellegrin Hospital, Inserm, UMR-1053, Bordeaux, France

CORRESPONDING AUTHOR:

Christine Sempoux, Service of Clinical Pathology, Lausanne University Hospital, Institute of Pathology. Rue du Bugnon 25 CH-1011 Lausanne. Tel. +41 21 314 7170, Fax: +41 21 314 7115. Email: christine.sempoux@chuv.ch.

LIST OF ABBREVIATIONS:

FNH: focal nodular hyperplasia

HCA: hepatocellular adenoma

H-HCA: *HNF1A* inactivated HCA

IHCA: inflammatory HCA

B-HCA: beta-catenin activated HCA

B-IHCA: beta-catenin activated inflammatory HCA

ASS1+HCA: argininosuccinate synthase 1 HCA

HCA-HCC: hepatocellular adenoma- hepatocellular carcinoma

MRI: magnetic resonance imaging

Gd-EOB- DTPA: gadolinium-ethoxybenzyl-diethylenetriamine penta-acetic acid

CONFLICTS OF INTEREST: None

FINANCIAL SUPPORT: Authors have nothing to disclose.

KEY POINTS

- FNH and HCA own different tissue expression of hepatocyte transporters involved in Gd-EOB-DTPA-enhanced MRI pharmacodynamics
- HCA with lower and higher risk of malignant transformation and HCA-HCC have specific hepatocyte transporters expression profiles
- Translational radiological criteria based on Gd-EOB-DTPA uptake can help to stratify HCA according to their risk of malignant transformation

Abstract

Background & Aims: Hepatobiliary phase (HBP) Gd-EOB-DTPA-enhanced magnetic resonance imaging (MRI) has increased the accuracy in differentiating focal nodular hyperplasia (FNH) and hepatocellular adenoma (HCA). However, the ability of this technique to distinguish HCA subtypes remains controversial. The aim of this study was to investigate the expression of hepatocyte transporters (OATPB1/B3, MRP2, MRP3) in HCA subtypes, hence to understand their MRI signal intensity on HBP Gd-EOB-DTPA-enhanced MRI.

Methods: By means of immunohistochemistry (IHC) we scored the expression of OATPB1/B3, MRP2 and MRP3, in resected specimens of FNH (n=40), subtyped HCA (n=58) and in HCA with focal malignant transformation (HCA-HCC, n=4). Results were validated on a supplementary set of FNH (n=6), subtyped HCA (n=17) and HCA-HCC (n=1) with Gd-EOB-DTPA MR images.

Results: All FNH showed a preserved expression of hepatocytes transporters. Beta-catenin activated HCA (at highest risk of malignant transformation) and HCA-HCC were characterized by preserved/increased OATPB1/B3 expression (predictor of hyperintensity on HBP), as opposed to other HCA subtypes ($p < 0.01$) that mostly showed OATPB1/B3 absence (predictor of hypointensity on HBP). HCA-HCC showed an additional MRP3 overexpressed profile ($p < 0.01$). On HBP Gd-EOB-DTPA-enhanced MRI, FNH and HCA signal intensity reflected the profile predicted by their specific OATPB1/B3 tissue expression. The hyperintense vs. hypointense HBP signal criterion was able to distinguish all higher risk HCA and HCA-HCC (100% accuracy).

Conclusions: OATPB1/B3 and MRP3 IHC and signal intensity on HBP Gd-EOB-DTPA-enhanced MRI can help to stratify HCA according to their risk of malignant transformation.

KEYWORDS: Hepatocellular adenoma, radio-pathological correlation, hepatocyte transporters, hepatospecific magnetic resonance imaging.

Introduction

Focal nodular hyperplasia (FNH) and hepatocellular adenoma (HCA), the two prototypical benign hepatocellular nodules, share common clinical context (child bearing women, history of oral contraception) and liver background (normal or non-cirrhotic).¹⁻⁴ However, unlike FNH, HCA is a true neoplastic process, entailing risk of bleeding and malignant transformation.^{5,6} In the last two decades, the oncogenic mechanisms activated in HCA have been characterized with molecular biology techniques, generating gene signatures translated in a molecular classification.⁷⁻¹⁰

According to the latter, HCA is divided into 4 subgroups, showing specific morphology, immunohistochemical phenotype, molecular background, clinical settings and natural history: *HNF1a* inactivated HCA (H-HCA), inflammatory HCA (IHCA) b-catenin activated HCA (b-HCA), and argininosuccinate synthase 1-positive/sonic hedgehog HCA (ASS1+HCA).^{8,11-13} H-HCA without classical steatosis (atypical H-HCA), mixed b-catenin activated and inflammatory HCA (b-IHCA) and HCA with focal transformation into hepatocellular carcinoma (HCA-HCC) are also observed. B-HCA and b-IHCA own the highest risk of malignant transformation due to their b-catenin (*CTNBB1*) exon 3 gene mutation, with a reported odds ratio of 9.3.^{12,14}

Therefore, the differential diagnosis between FNH and HCA, and a correct classification of HCA subtype, are important for a tailored management strategy.^{15,16}

In the current clinical practice, this task is mainly based on radiology, with magnetic resonance imaging (MRI) being the most valuable tool, and liver biopsy only performed in case of doubt.¹⁷⁻²⁰ However, MRI is less effective in the characterization of the HCA subtype (85% of correct diagnosis in the most performant series), prompting liver biopsy and pathological analysis, or proceed towards resection with the sole criterion of >5cm lesion size in a significant fraction of cases.^{17,21}

The introduction of hepatobiliary phase (HBP) Gd-EOB-DTPA-enhanced MRI has improved the diagnostic performance in the differential diagnosis of HCA vs. FNH, with a reported 91-100% sensitivity and 87-100% specificity.²²⁻²⁵ Gd-EOB-DTPA is a hepatospecific contrast agent transported through hepatocytes by hepatocyte transporters proteins (HT), namely organic anion-transporting polypeptides B1/B3 (OATPB1/B3) and multidrug resistance associated proteins 2 and 3 (MRP2, MRP3).²⁶ OATPB1/B3 is expressed at hepatocytes basolateral pole and allows the

contrast agent influx/backflux from and to the sinusoidal space; MRP3 is also expressed at the basolateral pole, allowing a complementary sinusoidal backflux; MRP2 is expressed at hepatocytes canalicular pole and is responsible of biliary efflux.

^{27,28} At imaging, FNH accumulates Gd-EOB-DTPA during the HBP (data acquisition at 20 minutes after venous injection), showing iso or hyperintensity as compared to the surrounding liver.^{27,29,30} By contrast, according to the literature, the HCA Gd-EOB-DTPA uptake profile is controversial. Only a few studies aimed to elucidate this phenomenon, showing mostly a hypointense profile.^{27,29-32} In a recent radiopathological report, it has been suggested that, in HCA, the degree of OATPB1/B3 and MRP3 expression correlated respectively with Gd-EOB-DTPA “retention” and “washout” seen on HBP MR images.³³ However, a precise pathological aracterization of HT expression patterns in HCA subtype according to the most recent classification, particularly in HCA with less common phenotypes (atypical H-HCA, ASS1+HCA), and with higher risk of malignant transformation (b-IHCA, b-HCA) and HCA-HCC is unclear. Aim of this study was to detail the expression of HT in FNH and HCA subtypes, and to investigate their signal intensity on HBP Gd-EOB-DTPA-enhanced MRI.

Materials and Methods

Cases under study

Study set: to characterize the HT expression of FNH and HCA, we collected 102 hepatocellular nodules (40 FNH, 58 HCA, 4 HCA-HCC), resected from 95 non-cirrhotic patients between 1995 and 2016. Material and clinical information were retrieved from the archives of Policlinico Maggiore, San Paolo, Istituto Europeo di

Oncologia and Istituto Nazionale dei Tumori hospitals (Milan, Italy) and Pellegrin Hospital (Bordeaux, France). Two liver pathologists reviewed all the original materials at the Lausanne University Hospital and classified nodules as FNH or HCA, then subtyped HCA with immunohistochemistry according to the most recent classification.^{8,13}

Validation set: to verify the Gd-EOB-DTPA intensity predicted by the study set results we reviewed 6 FNH, 17 HCA and 1 HCA-HCC from Lausanne University Hospital, comparing their preoperative hepatospecific MRI with postoperative pathological classification.

The diagnosis of HCA-HCC was retained only in cases with presence of evident HCC in otherwise undoubtful HCA. Evident HCC showed a combination of severe cytological atypia, thick (>3 hepatocytes) cell plates and prominent pseudoacinar architecture with bile plugs, in association with loss of the reticulin framework. The study protocol was in accordance with the recommendations of national and cantonal ethical committees and with the declaration of Helsinki. For Italian centers, informed consent and ethical committees approval was unneeded (G.U. 72 26 March 2012). For Pellegrin Hospital, patients informed consent and ethics approval by the local committee of "Direction de la Recherche Clinique et de l'Innovation" (Bordeaux University Hospital, Bordeaux, France; Liver Biobank of CHU Bordeaux, n° BRIF: BB-0033-00036) were obtained. For the Lausanne University Hospital, the Institutional Review Board and Human Research Ethics Committee of the University Hospital of Lausanne, Switzerland approved this retrospective study and patients' active consent was waived (protocol 483/13).

Immunohistochemistry

For all cases, centers involved in the study provided three consecutive recuts from the original paraffin blocks that were stained with antibodies against OATPB1/B3, MRP2 and MRP3 (detailed in Table S1), following standard procedures. In all specimens, extralesional liver tissue was available for the pathological analysis and served as internal positive control. Two observers (C.S., A.S.) independently assessed the HT staining on each nodule. Consensus was obtained after discussion at multihead microscope in discordant cases. The HT staining pattern was descriptively reported and a semiquantitative evaluation was performed according to the following criteria: 0= HT not expressed, as opposed to adjacent non tumoral liver; 1= HT expressed similarly to adjacent liver; 2= HT increased expression as compared to the adjacent liver. Fig. S1 illustrates visual references for this semiquantitative analysis.

Gd-EOB-DTPA-enhanced MR image analysis

Unaware of the results of the pathological study set cases, an expert radiologist, with 15 years experience in liver MRI (S.S.) reviewed Gd-EOB-DTPA-enhanced MR images of the validation set cases. Each nodule was visually classified on HBP as being either hypointense, isointense or hyperintense in comparison with the surrounding liver parenchyma.

Statistical Analysis

Variables were reported as numbers and percentages and summarized as mean (\pm SD) or median with interquartile range (IQR). We compared groups using the Mann-Whitney, χ^2 or Fisher exact tests, as appropriate. Tests were two-sided and we used

a significance level of 0.05. Analyses were performed with R software and SPSS 23.0 (©2013 SPSS Inc., Chicago, IL, USA).

Results

Clinico-pathological data

The 95 study set patients were mostly female (88%), with a median age of 37 years (IQR 11), all without history of previous primary liver tumor. Clinically, a fraction of patients showed metabolic (19%) or circulation (17%) disorders. History of oral contraception was recorded in 35/84 (42%) female patients. For diagnostic purpose, in most cases, two or more imaging techniques were used, with CT and non-hepatospecific MRI performed in 79/95 (83%) cases. At pathological analysis (resected specimens), fatty or vascular liver disease was observed in 34/95 (36%) cases, while no patient showed advanced fibrosis, cirrhosis or chronic liver disease of other origins. Median pathological lesional size was 3 cm (IQR 8.3). As compared to FNH, HCA grouped more patients with OC history (51% vs. 17%, $p=0.001$), multiple (44% vs. 15%, $p=0.003$) and larger lesions (5.8 vs. 4 cm, $p=0.009$). Clinico-pathological parameters according to FNH or HCA diagnosis in the study set are indicated in Table 1. Clinico-pathological parameters of 24 patients included in the validation set did not significantly differed from the study set ones (data not shown).

HCA subtyping

Study set (n=62): 24 H-HCA (38.7%), 4 atypical H-HCA (6.5%), 15 IHCA (24.2%), 4 ASS1+HCA (6.4%), 5 b-HCA (8.1%), 6 b-IHCA (9.7%), and 4 HCA-HCC (6.4%). HCA-HCC originated from b-HCA in 3 cases and b-IHCA in one case.

Validation set (n=18): 3 H-HCA, 8 IHCA, 4 ASS1+HCA, 2 b-HCA, and 1 HCA-HCC originating from a b-HCA.

Beta-catenin activated HCA displayed strong glutamine synthetase staining congruent with *CTNNB1* exon 3 mutations.

Study set: HT expression in FNH vs. HCA

All FNH expressed the three HT, with a periseptal staining pattern. HT staining was similar to adjacent extralesional liver tissue (score=1), but more diffuse in hepatocytes at the interface with fibrosis. The subcellular pattern was preserved (OATPB1/B3 and MRP3 basolateral, MRP2 apical), but an extension to other parts of the cell membrane could be observed for OATPB1/B3 and MRP3 in the periseptal area. Ductular reaction was strongly immunoreactive for MRP2 and MRP3. Fig. 1 illustrates HT expression in FNH. In HCA, the three HT expression was variable, either lost, present or increased (score 0, 1 or 2), significantly differing from FNH ($p<0.001$). When HT were present, the subcellular pattern of staining could be modified (not polarized, without specific topographical distribution on cell membrane). Notably, the majority (71%) of cases were OATPB1/B3 negative. HT expression in FNH and HCA is summarized in Table 2. In the adjacent liver, HT staining was preserved in all cases (internal positive control), not modified even in presence of vascular or fatty liver disease.

Study set: HT expression in HCA subtypes

Typical and atypical H-HCA (n=28) showed similar OATPB1/B3 loss (100% score=0). MRP2 was also mostly lost in both groups (87% and 75% score=0)

whereas a remarkably different MRP3 expression was observed (score=0 in 92% of typical vs. 25% of atypical H-HCA, $p=0.025$).

IHCA (n=15) showed OATPB1/B3 loss in a majority of the cases (86.7% score=0) while MRP2 and MRP3 expression was preserved or increased (100% score=1 or 2, for both). ASS1+HCA (n=4), showed OATPB1/B3 and MRP3 loss in a majority of the cases (75% score=0), and preserved MRP2 expression (100% score=1). HT expression in these subgroups of HCA at lower risk of malignant transformation is illustrated in Fig. 2.

HCA with higher risk of malignant transformation (b-HCA, b-IHCA) presented a preserved or increased OATPB1/B3 expression: b-HCA (n=5, 100% score=2), b-IHCA (n=6, 100% score=1 or 2). By contrast with FNH, the preserved OATPB1/B3 (score 1) expression in 4 b-IHCA, as well as in 2 IHCA, was more diffuse, with no enhancement in the hepatocytes located at the interface with fibrosis (pseudo-portal tracts).

MRP2 was always present (100% score =1 or 2) and MRP3 was lost in b-HCA (100% score=0) and preserved in b-IHCA (100% score=1).

Finally, HCA-HCC (n=4) showed increased OATPB1/B3 expression (100% score=2), preserved or increased MRP2 expression (100% score 1 or 2) and mostly increased MRP3 expression (66% score 2). HT profile of higher risk HCA and HCA-HCC is illustrated in Fig. 3 and HT expression for all HCA subtypes is detailed in Table 3.

Thus, OATPB1/B3 score=1 or 2 (predictive of hyperintense HBP) was suggestive of HCA with higher risk of malignant transformation ($p<0.001$) and the association of OATPB1/B3 score=2 (predictive of hyperintense signal on HBP MR images) with additional MRP3 score=2 (predictive of Gd-EOB-DTPA retention at HBP) was

suggestive of HCA-HCC ($p < 0.001$). A scheme of the expected radiological findings in HCA subtypes derived from our results is illustrated in Fig. 4.

Validation Set

All FNH were iso/hyperintense on HBP Gd-EOB-DTPA-enhanced MR images compared to the adjacent liver due to intracellular contrast agent uptake. Intensity was mostly heterogeneous, reflecting the presence of intralesional fibrous septa. All H-HCA, IHCA and ASS1+HCA were hypointense on HBP due to the absence of intracellular Gd-EOB-DTPA uptake. The two b-HCA and the one HCA-HCC were hyperintense on HBP Gd-EOB-DTPA-enhanced MR images as compared to adjacent liver. Accordingly, HBP Gd-EOB-DTPA-enhanced MRI was able to identify HCA at higher risk for malignancy with a sensitivity, specificity and accuracy of 100%. Examples of the HBP Gd-EOB-DTPA MRI features of FNH, HCA and HCA-HCC from the validation set are illustrated in Fig. 5.

Discussion

In this study, we focused on the translational use of HT expression to clarify the features of FNH and HCA observed on the HBP of Gd-EOB-DTPA-enhanced MRI. Our working hypothesis was that the reported controversial MRI findings in HCA might rely on a different HT expression according to HCA subtype. To our knowledge, this is the first study aimed to outline HT expression in a large series of resected FNH and HCA, classified with updated criteria, including rare subtypes and with an independent external radio-pathological validation set.

We observed that HT expression in FNH is characterized by a periseptal pattern, with little variation in different cases, matching the iso/hyperintense contrast uptake

on the HBP of Gd-EOB-DTPA-enhanced MRI that is consistently reported in the literature.^{24,25,27,30,32,34} By contrast, in HCA, HT expression is heterogeneous, resulting in a variable intracellular uptake of the hepatospecific contrast agent.²⁷ Our results refine those reported in a previous study, based on outdated pathological classifications, showing consistently low OATPB1/B3 mRNA levels and IHC expression in 9 HCA.³¹ Independently from the subtype, we noted that approximately 70% of HCA did not display OATPB1/B3 expression. Thus, our results suggest that the “no HBP uptake” criterion proposed in several radiological papers is indeed generally helpful to separate FNH from the majority of HCA.^{32,35,36} These observations are in accordance with those reported in a systematic review, showing that FNH have iso- or high signal, while most HCA have low signal on HBP as compared to the background liver.²³ These authors also suggested that the hypersignal in FNH is due to higher expression of OATP transporters as compared to HCA, which is confirmed by the present study.²³

In accordance with a previous report by Fukusato et al., when HT profile was investigated in different HCA subtypes, we found that in HCA at higher risk of malignant transformation (b-IHCA, b-HCA) and in HCA-HCC, OATPB1/B3 expression is present or increased, as compared to the adjacent liver.³⁷ This result can be of translational interest, as OATPB1/B3 staining could be helpful in stratifying HCA according to their risk of malignancy. As such, OATPB1/B3 staining on a liver nodule could potentially be a supplementary tool in tailoring the patient management. In the study set, H-HCA, typical and atypical, showed a homogenous loss of OATPB1/B3. This subcategory of atypical H-HCA, characterized at the histological level by loss of steatosis and focal pseudoglandular architecture, is not well understood. By contrast to typical H-HCA, the increased MRP3 expression that we

found in this entity underlines a specificity deserving further investigation. Similarly, all but 2 IHCA showed loss of OATPB1/B3 expression. The persistence of OATPB1/B3, paired with consistent presence of MRP2 and MRP3 expression in a few IHCA and more frequently b-IHCA, suggest that a few of them can have an imaging overlap with FNH, somehow recalling the outdated nomenclature of IHCA as “telangiectatic FNH”.³⁸ The final diagnosis of IHCA and b-IHCA rely on a multimodal approach, including conventional morphology and immunohistochemistry. In addition, in IHCA and b-IHCA with preserved (score 1) OATPB1/B3 expression, the pattern of staining differed from the one of FNH, which was enhanced in periseptal areas.

Little is known on the clinical behavior of ASS1+HCA, except for their predisposition to bleeding.^{12,13} The majority of them in this study showed loss of OATPB1/B3, grouping them with H-HCA and IHCA.

We then validated these observations in an independent cohort with radio-pathological data. In these patients, the Gd-EOB-DTPA uptake profile was congruent with the one predicted by the study set results: FNH were all iso/hyperintense, HCA at higher risk of malignant transformation showed hyperintense signal and other HCA were characterized by a hypointense signal. These findings, even if based on a relatively limited number of observations, suggest that signal intensity may be a surrogate marker of OATPB1/B3 presence or loss. In agreement with our results, Ba-Ssalamah et al. reported Gd-EOB-DTPA “retention” in 83% of b-HCA on the HBP of Gd-EOB-DTPA-enhanced MRI, while they inconsistently observed this hyperintensity in other HCA subtypes.³³ However, this series did not include all subtypes. Recently, Reizine et al. reported similar results with a signal intensity quantitative analysis on Gd-BOPTA imaging.³⁹ Since high-risk HCA showed a

hyperintense signal on the HBP of Gd-EOB-DTPA-enhanced MR images in our study, the radiological differentiation from hyperintense FNH should also rely on other MRI features, such as the heterogeneous “periseptal” uptake of FNH on HBP, the presence of a central scar, or other MR phases features. Indeed, unlike FNH, b-HCA typically demonstrate a subtle heterogenous hypersignal on T2-weighted MR images.³³ In some cases, the final answer will require the pathological analysis of a biopsy.²⁰

The molecular mechanism underpinning OATPB1/B3 expression (and finally HBP hyperintense signal) in HCA at higher risk of malignancy has not yet been investigated. A review of the MR features seen on HBP in benign hepatocellular nodules suggested a mechanistic link between the activation of the Wnt/b-catenin pathway and OATPB1/B3 expression based on experimental studies on animal models.⁴⁰⁻⁴² This potential link seems really appealing, as the activation of this molecular pathway could explain the hyperintense signal observed in FNH (non-mutant Wnt/ b-catenin activation), b-IHCA and b-HCA (mutant Wnt/ b-catenin activation).⁴⁰

The functional role of MRP2 and MRP3 in FNH and HCA is more controversial. Their activity is expected to rely on OATPB1/B3 function (no efflux and backflux without uptake) and the reported absence of physiological connection with the biliary tree in FNH and HCA suggests that no biliary efflux through MRP2 is possible.^{31,33} MRP3 can be involved in the hepatospecific contrast agent release into the sinusoids of hyperintense hepatocellular lesions. In our series, all HCA-HCC showed OATPB1/B3 expression and, in two cases, increased MRP3 expression was also found, suggesting a shorter retention of hepatospecific contrast agent in these lesions. As

HCA-HCC are early malignant lesions, our results seem in accordance with those of Kitao et al., who suggested that OATPB1/B3 expression decreases with tumor dedifferentiation, being more intense in early stage HCC.^{43,44} To date, no evidence is available to clarify the reason of MRP3 expression in HCA-HCC, but the MRP3 overexpression reported in cholestatic liver disease can draw an intriguing link between MRP3 expression and cholestatic features (such as bile thrombi formation) observed in HCA-HCC.^{26,45} Interestingly, in mouse models, it has been shown that the hepatocyte-specific expression of an oncogenic variant of b-catenin (originated through exon 3 deletion of *CTNBB1*, comparable to mutant exon 3 *CTNBB1* of human b-HCA), results in cholestatic liver disease and eventually therefore to increased MRP3 expression.^{46,47}

In conclusion, our results suggest that the tissue expression of HT in FNH and HCA subtypes correlates with signal intensity observed on HBP of Gd-EOB-DTPA-enhanced MRI. In HCA, the signal intensity at HBP together with the immunohistochemical staining for OATPB1/B3 and MRP3, that remains to be validated on biopsies, could be useful in identifying HCA at risk of malignant transformation and help in stratifying patient for a tailored management. Our results, in particular the radio-pathological comparison, should be further validated, especially in the light of the low number of cases for some HCA subtypes. This validation study should prospectively compare the hepatospecific MR features and the expression of hepatocyte transporters in biopsies of a large series of HCA, specifically focusing on higher risk lesions, in close comparison with their clinical follow-up.

References

1. Roncalli M, Sciarra A, Tommaso LD. Benign hepatocellular nodules of healthy liver: focal nodular hyperplasia and hepatocellular adenoma. *Clin Mol Hepatol*. 2016;22(2):199-211.
2. Sempoux C, Paradis V, Komuta M, et al. Hepatocellular nodules expressing markers of hepatocellular adenomas in Budd-Chiari syndrome and other rare hepatic vascular disorders. *J Hepatol*. 2015;63(5):1173-1180.
3. Dokmak S, Paradis V, Vilgrain V, et al. A single-center surgical experience of 122 patients with single and multiple hepatocellular adenomas. *Gastroenterology*. 2009;137(5):1698-1705.
4. Chang CY, Hernandez-Prera JC, Roayaie S, Schwartz M, Thung SN. Changing epidemiology of hepatocellular adenoma in the United States: review of the literature. *Int J Hepatol*. 2013;2013:604860.
5. Paradis V, Laurent A, Flejou JF, Vidaud M, Bedossa P. Evidence for the polyclonal nature of focal nodular hyperplasia of the liver by the study of X-chromosome inactivation. *Hepatology*. 1997;26(4):891-895.
6. Chen YJ, Chen PJ, Lee MC, Yeh SH, Hsu MT, Lin CH. Chromosomal analysis of hepatic adenoma and focal nodular hyperplasia by comparative genomic hybridization. *Genes Chromosomes Cancer*. 2002;35(2):138-143.
7. Zucman-Rossi J, Jeannot E, Nhieu JT, et al. Genotype-phenotype correlation in hepatocellular adenoma: new classification and relationship with HCC. *Hepatology*. 2006;43(3):515-524.
8. Bioulac-Sage P, Rebouissou S, Thomas C, et al. Hepatocellular adenoma subtype classification using molecular markers and immunohistochemistry. *Hepatology*. 2007;46(3):740-748.
9. Sasaki M, Yoneda N, Kitamura S, Sato Y, Nakanuma Y. Characterization of hepatocellular adenoma based on the phenotypic classification: The Kanazawa experience. *Hepatology research : the official journal of the Japan Society of Hepatology*. 2011;41(10):982-988.
10. Bellamy CO, Maxwell RS, Prost S, Azodo IA, Powell JJ, Manning JR. The value of immunophenotyping hepatocellular adenomas: consecutive resections at one UK centre. *Histopathology*. 2013;62(3):431-445.
11. Bioulac-Sage P, Balabaud C, Bedossa P, et al. Pathological diagnosis of liver cell adenoma and focal nodular hyperplasia: Bordeaux update. *J Hepatol*. 2007;46(3):521-527.
12. Nault JC, Couchy G, Balabaud C, et al. Molecular Classification of Hepatocellular Adenoma Associates With Risk Factors, Bleeding, and Malignant Transformation. *Gastroenterology*. 2017;152(4):880-894.e886.
13. Henriot E, Abou Hammoud A, Dupuy JW, et al. Argininosuccinate synthase 1 (ASS1): A marker of unclassified hepatocellular adenoma and high bleeding risk. *Hepatology*. 2017;66(6):2016-2028.
14. Bioulac-Sage P, Laumonier H, Couchy G, et al. Hepatocellular adenoma management and phenotypic classification: the Bordeaux experience. *Hepatology*. 2009;50(2):481-489.
15. Cho SW, Marsh JW, Steel J, et al. Surgical management of hepatocellular adenoma: take it or leave it? *Annals of surgical oncology*. 2008;15(10):2795-2803.
16. Cherqui D, Rahmouni A, Charlotte F, et al. Management of focal nodular hyperplasia and hepatocellular adenoma in young women: a series of 41 patients with clinical, radiological, and pathological correlations. *Hepatology*. 1995;22(6):1674-1681.
17. Ronot M, Bahrami S, Calderaro J, et al. Hepatocellular adenomas: accuracy of magnetic resonance imaging and liver biopsy in subtype classification. *Hepatology*. 2011;53(4):1182-1191.
18. Agnello F, Ronot M, Valla DC, Sinkus R, Van Beers BE, Vilgrain V. High-b-value diffusion-weighted MR imaging of benign hepatocellular lesions: quantitative and qualitative analysis. *Radiology*. 2012;262(2):511-519.

19. Laumonier H, Bioulac-Sage P, Laurent C, Zucman-Rossi J, Balabaud C, Trillaud H. Hepatocellular adenomas: magnetic resonance imaging features as a function of molecular pathological classification. *Hepatology*. 2008;48(3):808-818.
20. EASL Clinical Practice Guidelines on the management of benign liver tumours. *J Hepatol*. 2016;65(2):386-398.
21. Nault JC, Bioulac-Sage P, Zucman-Rossi J. Hepatocellular benign tumors-from molecular classification to personalized clinical care. *Gastroenterology*. 2013;144(5):888-902.
22. Grazioli L, Bondioni MP, Haradome H, et al. Hepatocellular adenoma and focal nodular hyperplasia: value of gadoxetic acid-enhanced MR imaging in differential diagnosis. *Radiology*. 2012;262(2):520-529.
23. McInnes MD, Hibbert RM, Inacio JR, Schieda N. Focal Nodular Hyperplasia and Hepatocellular Adenoma: Accuracy of Gadoxetic Acid-enhanced MR Imaging--A Systematic Review. *Radiology*. 2015;277(2):413-423.
24. Tselikas L, Pigneur F, Roux M, et al. Impact of hepatobiliary phase liver MRI versus Contrast-Enhanced Ultrasound after an inconclusive extracellular gadolinium-based contrast-enhanced MRI for the diagnosis of benign hepatocellular tumors. *Abdom Radiol (NY)*. 2017;42(3):825-832.
25. Roux M, Pigneur F, Baranes L, et al. Differentiating focal nodular hyperplasia from hepatocellular adenoma: Is hepatobiliary phase MRI (HBP-MRI) using linear gadolinium chelates always useful? *Abdom Radiol (NY)*. 2017.
26. Boyer JL. Bile formation and secretion. *Comprehensive Physiology*. 2013;3(3):1035-1078.
27. Van Beers BE, Pastor CM, Hussain HK. Primovist, Eovist: what to expect? *J Hepatol*. 2012;57(2):421-429.
28. Leporq B, Daire JL, Pastor CM, et al. Quantification of hepatic perfusion and hepatocyte function with dynamic gadoxetic acid-enhanced MRI in patients with chronic liver disease. *Clinical science (London, England : 1979)*. 2018;132(7):813-824.
29. Denecke T, Steffen IG, Agarwal S, et al. Appearance of hepatocellular adenomas on gadoxetic acid-enhanced MRI. *European radiology*. 2012;22(8):1769-1775.
30. Grieser C, Steffen IG, Kramme IB, et al. Gadoxetic acid enhanced MRI for differentiation of FNH and HCA: a single centre experience. *European radiology*. 2014;24(6):1339-1348.
31. Vander Borght S, Libbrecht L, Blokzijl H, et al. Diagnostic and pathogenetic implications of the expression of hepatic transporters in focal lesions occurring in normal liver. *J Pathol*. 2005;207(4):471-482.
32. Guo Y, Li W, Cai W, Zhang Y, Fang Y, Hong G. Diagnostic Value of Gadoxetic Acid-Enhanced MR Imaging to Distinguish HCA and Its Subtype from FNH: A Systematic Review. *Int J Med Sci*. 2017;14(7):668-674.
33. Ba-Ssalamah A, Antunes C, Feier D, et al. Morphologic and Molecular Features of Hepatocellular Adenoma with Gadoxetic Acid-enhanced MR Imaging. *Radiology*. 2015;277(1):104-113.
34. Grieser C, Steffen IG, Seehofer D, et al. Histopathologically confirmed focal nodular hyperplasia of the liver: gadoxetic acid-enhanced MRI characteristics. *Magn Reson Imaging*. 2013;31(5):755-760.
35. Thomeer MG, ME EB, de Lussanet Q, et al. Genotype-phenotype correlations in hepatocellular adenoma: an update of MRI findings. *Diagnostic and interventional radiology (Ankara, Turkey)*. 2014;20(3):193-199.
36. Suh CH, Kim KW, Kim GY, Shin YM, Kim PN, Park SH. The diagnostic value of Gd-EOB-DTPA-MRI for the diagnosis of focal nodular hyperplasia: a systematic review and meta-analysis. *European radiology*. 2015;25(4):950-960.
37. Fukusato T, Soejima Y, Kondo F, et al. Preserved or enhanced OATP1B3 expression in hepatocellular adenoma subtypes with nuclear accumulation of beta-catenin. *Hepatology research : the official journal of the Japan Society of Hepatology*. 2015;45(10):E32-42.

38. Paradis V, Benzekri A, Dargere D, et al. Telangiectatic focal nodular hyperplasia: a variant of hepatocellular adenoma. *Gastroenterology*. 2004;126(5):1323-1329.
39. Reizine E, Amaddeo G, Pigneur F, et al. Quantitative correlation between uptake of Gd-BOPTA on hepatobiliary phase and tumor molecular features in patients with benign hepatocellular lesions. *European radiology*. 2018.
40. Yoneda N, Matsui O, Kitao A, et al. Benign Hepatocellular Nodules: Hepatobiliary Phase of Gadoteric Acid-enhanced MR Imaging Based on Molecular Background. *Radiographics : a review publication of the Radiological Society of North America, Inc*. 2016;36(7):2010-2027.
41. Colletti M, Cicchini C, Conigliaro A, et al. Convergence of Wnt signaling on the HNF4alpha-driven transcription in controlling liver zonation. *Gastroenterology*. 2009;137(2):660-672.
42. Lu H, Gonzalez FJ, Klaassen C. Alterations in hepatic mRNA expression of phase II enzymes and xenobiotic transporters after targeted disruption of hepatocyte nuclear factor 4 alpha. *Toxicological sciences : an official journal of the Society of Toxicology*. 2010;118(2):380-390.
43. Kitao A, Zen Y, Matsui O, et al. Hepatocellular carcinoma: signal intensity at gadoteric acid-enhanced MR Imaging--correlation with molecular transporters and histopathologic features. *Radiology*. 2010;256(3):817-826.
44. Kitao A, Matsui O, Yoneda N, et al. The uptake transporter OATP8 expression decreases during multistep hepatocarcinogenesis: correlation with gadoteric acid enhanced MR imaging. *European radiology*. 2011;21(10):2056-2066.
45. Zollner G, Fickert P, Zenz R, et al. Hepatobiliary transporter expression in percutaneous liver biopsies of patients with cholestatic liver diseases. *Hepatology*. 2001;33(3):633-646.
46. Lemberger UJ, Fuchs CD, Karer M, et al. Hepatocyte specific expression of an oncogenic variant of beta-catenin results in cholestatic liver disease. *Oncotarget*. 2016;7(52):86985-86998.
47. Yeh TH, Krauland L, Singh V, et al. Liver-specific beta-catenin knockout mice have bile canalicular abnormalities, bile secretory defect, and intrahepatic cholestasis. *Hepatology*. 2010;52(4):1410-1419.

Figure legends

Fig. 1. Study set: hepatocyte transporters expression in FNH.

(A) At morphological analysis, FNH displayed intralesional fibrous septa, prominent ductular reaction and inflammation (H&E stain, 10x). (B-D) Hepatocyte transporters were systematically expressed in periseptal hepatocytes (B, OATPB1/B3 stain, 10x) (C, MRP2 stain, 10x) (D) MRP3 stain, 10x).

Fig. 2. Study set: hepatocyte transporters expression in HCA with lower risk of malignant transformation.

(A) At morphological analysis, this H-HCA shows typical steatotic features (H&E stain, 10x) and (B-D) is characterized by absence of hepatocyte transporters expression (B, OATPB1/B3 stain, 10x) (C, MRP2 stain, 10x) (D) MRP3 stain, 10x).

Fig. 3. Study set: hepatocyte transporters expression in HCA with higher risk of malignant transformation and in HCA-HCC.

(A) Hematoxylin-eosin example of b-HCA (left panel), and HCA-HCC displaying malignant features with rosettes formation and bile thrombi (right panel, arrows) (H&E stain, 10x). (B-C) The phenotype of these lesions was characterized by increased OATPB1/B3 expression (B, OATPB1/B3 stain, 10x) and presence of MRP2 expression (C, MRP2 stain, 10x). (D) In b-IHCA and b-HCA (left panel) no MRP3 expression was detectable, as opposed to the increased MRP3 expression observed in HCA-HCC (right panel) (MRP3 stain, 10x).

Fig. 4. Schematic representation of the expected radiological findings in HCA subtypes and HCA-HCC.

Based on our results, H-HCA, IHCA and ASS1+HCA are expected to show a hypointense signal on the HBP of Gd-EOB-DTPA-enhanced MRI, as contrast agent cannot enter into the hepatocytes due to absence of OATPB1/B3 expression. Conversely, b-HCA, b-IHCA and HCA-HCC are expected to show a hyperintense signal. A faster sinusoidal excretion might be observed in HCA-HCC because of their increased MRP3 expression.

Fig. 5. Validation set: examples of HBP Gd-EOB-DTPA MRI in FNH, HCA subtypes and HCA-HCC.

(A) FNH. These two (arrows) synchronous heterogeneously iso-hyperintense tumors were diagnosed as FNH at pathological analysis (B) FNH (arrowhead) and lower risk HCA (arrow). These two synchronous tumors, respectively heterogeneously hyperintense and hypointense, were diagnosed as FNH and IHCA at pathological analysis. (C) Higher risk HCA. This hyperintense tumor (arrow) was diagnosed as b-HCA at pathological analysis. (D) HCA-HCC. This centrally necrotic, hyperintense tumor (arrows) was diagnosed as HCA-HCC at pathological analysis.

Tables

Table 1. Clinico-pathological parameters according to the pathological diagnosis in the 102 hepatocellular nodules.

Variable	Category	FNH	HCA	p
Gender	Female	34 (85%)	57 (92%)	NS
	Male	6 (15%)	5 (8%)	
Age	Median (IQR)	37 (9.8)	37 (11.8)	NS
BMI	Median (IQR)	24 (4.2)	23 (5.6)	NS
OC	No	30 (83%)	29 (49%)	0.001
	Yes	6 (17%)	30 (51%)	
Metabolic disorder	No	32 (80%)	51 (82%)	NS
	Yes	8 (20%)	11 (18%)	
Circulation disorder	No	32 (80%)	53 (85%)	NS
	Yes	8 (20%)	9 (15%)	
Discovery	Asymptomatic	24 (60%)	41 (66%)	NS
	Symptomatic	16 (40%)	21 (34%)	
N. of radiological investigations	Median (IQR)	2.0 (0)	2.0 (1.0)	NS
Number of lesions	Single	34 (85%)	35 (56%)	0.003
	Multiple synchronous	6 (15%)	27 (44%)	
Size (cm)	Median (IQR)	4.0 (4.9)	5.8 (5.5)	0.009
Extraslesional liver morphology	Normal	28 (70%)	37 (56%)	NS
	Pathological	12 (30%)	25 (44%)	

Legend: BMI: Body mass index; OC: oral contraception.

Table 2. Expression score of hepatocyte transporters in FNH and HCA.

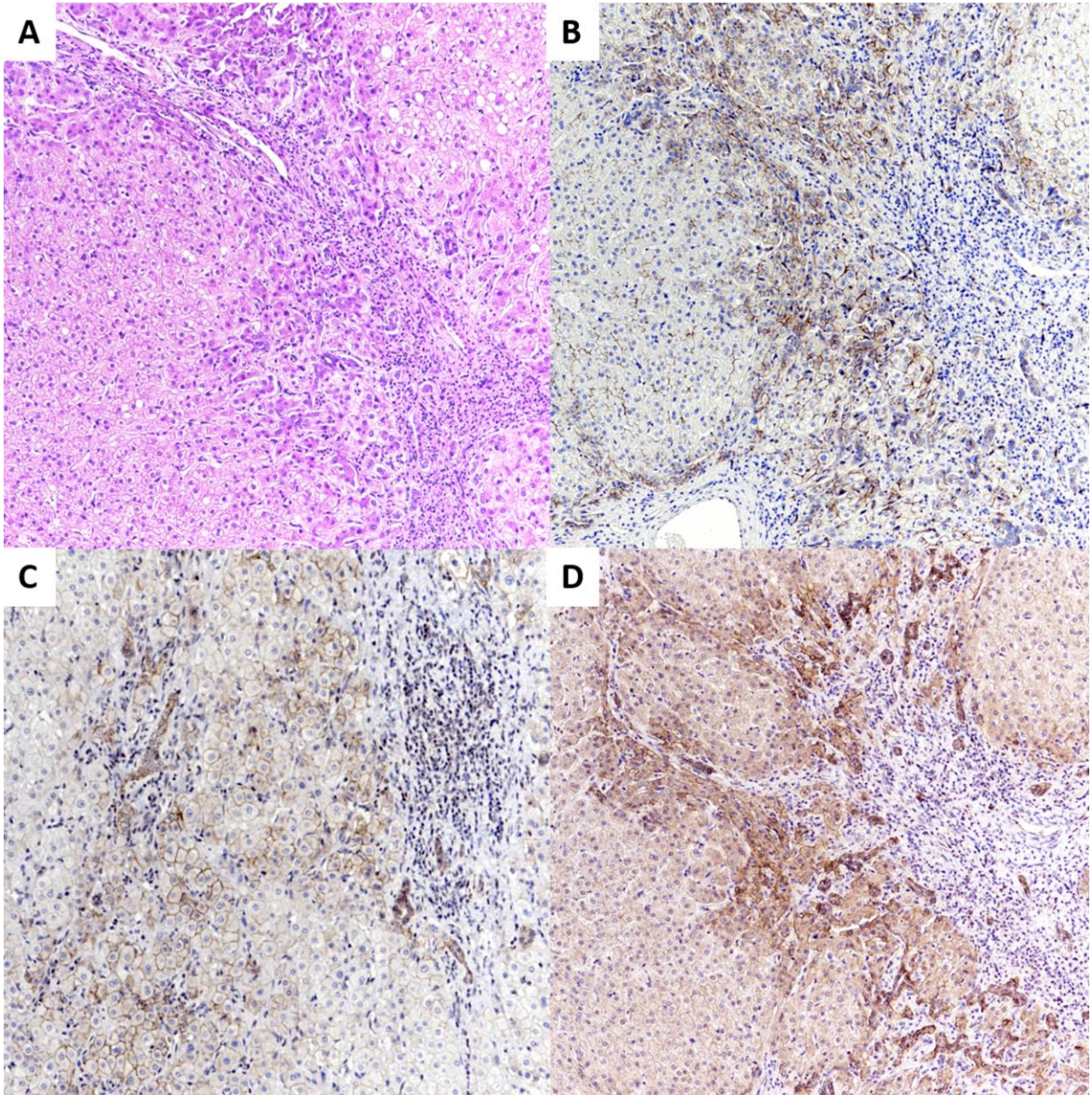
Variable	Score	FNH (n=40)	HCA (n=62)	P
OATPB1/B3*	1	40 (100%)	8 (13.3%)	<0.001
	0 or 2	0	52 (86.7%)	
MRP2	1	40 (100%)	28 (45.2%)	<0.001
	0 or 2	0	34 (54.8%)	
MRP3*	1	40 (100%)	18 (29.5%)	<0.001
	0 or 2	0	43 (70.5%)	

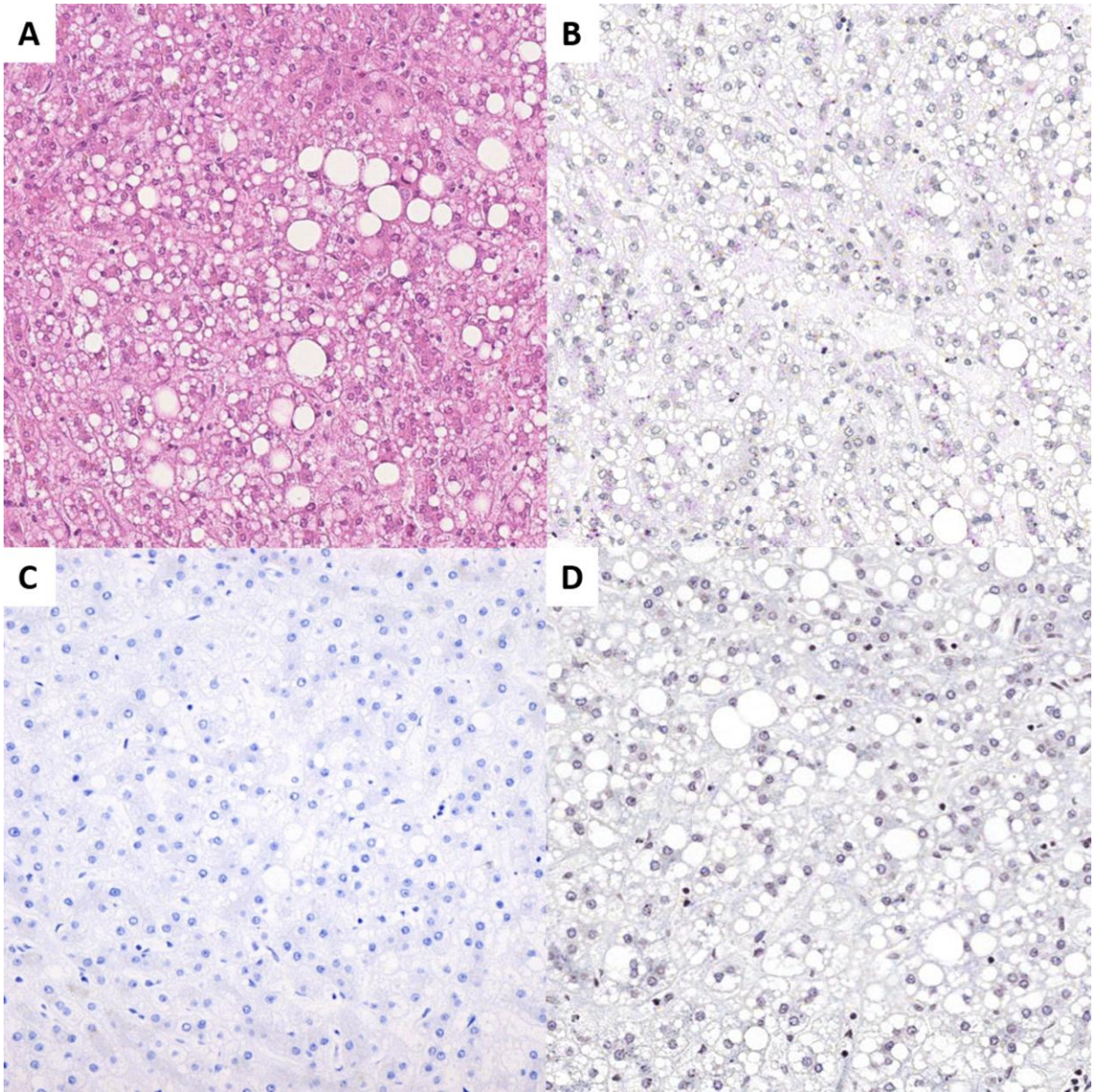
Legend: *: missing value for 2 HCA (OATPB1/B3) and 1 HCA (MRP3).

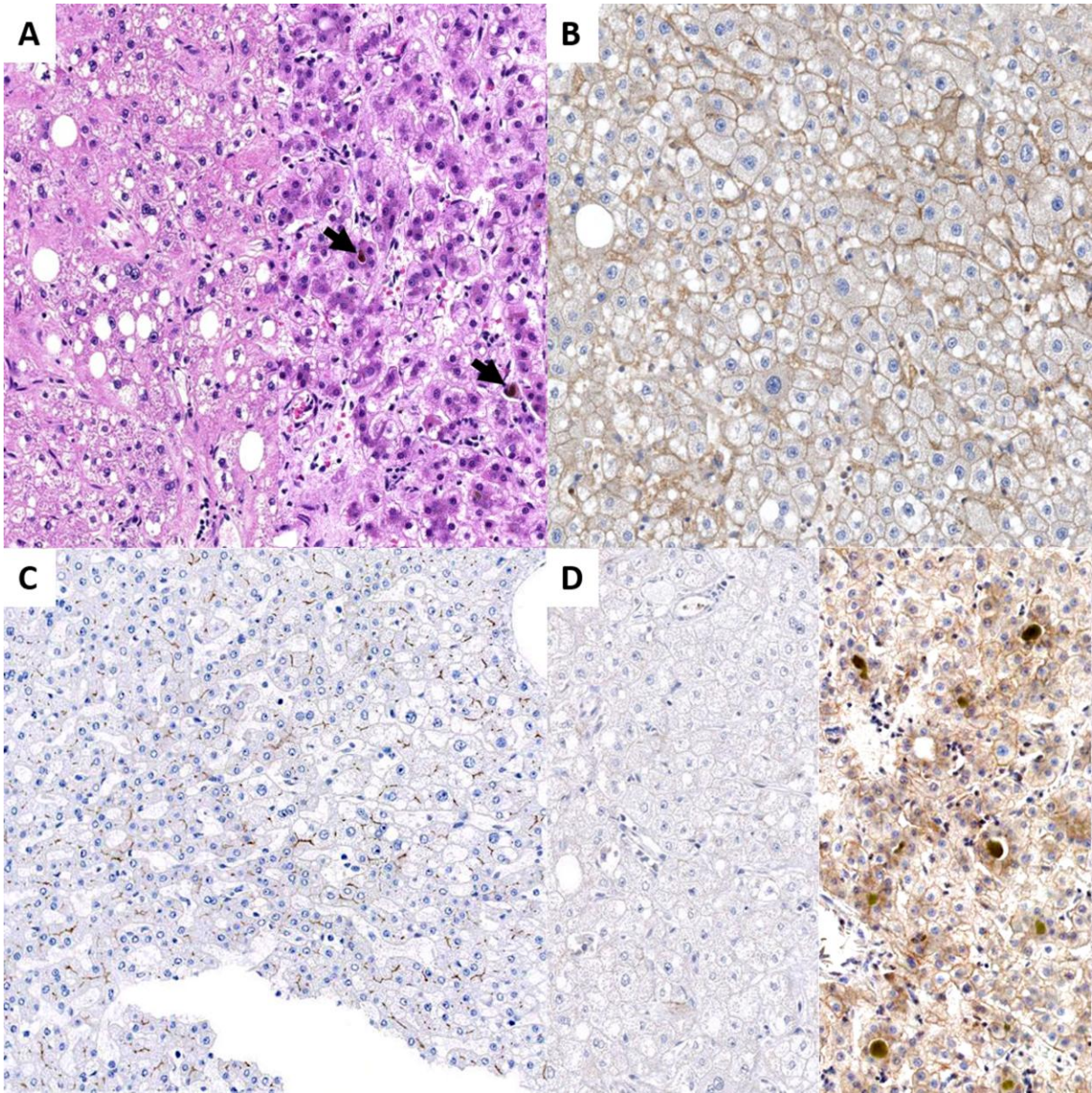
Table 3. Expression score of hepatocyte transporters in HCA subtypes and HCA-HCC (n=62).

Variable	Score	H-HCA (n=24)	Atypical H- HCA (n=4)	IHCA (n=15)	ASS1+HCA (n=4)	b-HCA (n=5)	b-IHCA (n=6)	HCA-HCC (n=4)
OATPB1/B3*	0	24 (100%)	4 (100%)	13 (86.7%)	3 (75%)	0	0	0
	1	0	0	2 (13.3%)	1 (25%)	0	4 (66.7%)	0
	2	0	0	0	0	5 (100%)	1 (33.3%)	3 (100%)
MRP2	0	21 (87.5%)	3 (75%)	0	0	0	0	0
	1	3 (12.5%)	1 (25%)	14 (93.3%)	4 (100%)	2 (40%)	3 (50%)	1 (25%)
	2	0	0	1 (6.7%)	0	3 (60%)	3 (50%)	3 (75%)
MRP3*	0	22 (92%)	1 (25%)	0	3 (75%)	5 (100%)	0	1 (33.3%)
	1	1 (4%)	0	11 (73.3%)	1 (25%)	0	6 (100%)	0
	2	1 (4%)	3 (75%)	4 (26.7%)	0	0	0	2 (66.7%)

Legend: *missing value for 1 b-IHCA, 1 HCA-HCC (OATPB1/B3) and 1 HCA-HCC (MRP3).

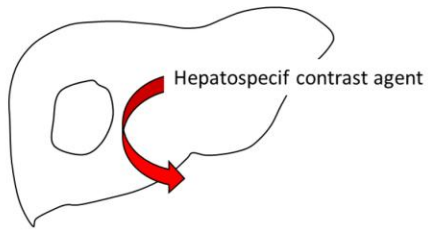






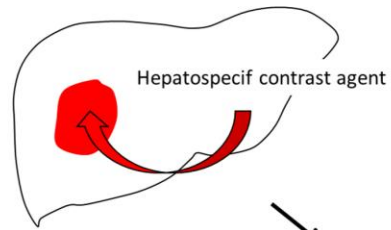
H-HCA, I-HCA, ASS1-HCA

OATPB1/B3 -



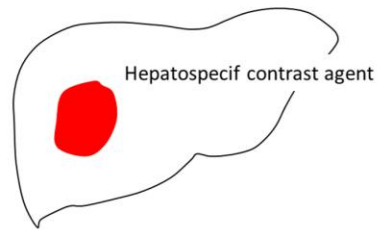
b-HCA, b-I-HCA, HCA-HCC

OATPB1/B3 +



b-HCA, b-I-HCA

MRP2 + MRP3 -



HCA-HCC

MRP2 + MRP3 +

